BY AHMAD A. MASOUD

Kinodynamic Motion Planning

A Novel Type of Nonlinear, Passive Damping Forces and Advantages

This article extends the capabilities of the harmonic potential field (HPF) approach to planning to cover both the kinematic and dynamic aspects of a robot's motion. The suggested approach converts the gradient guidance field from a harmonic potential to a control signal by augmenting it with a novel type of damping forces called nonlinear, anisotropic, damping forces (NADFs). The combination of the two provides a signal that can both guide a robot and effectively manage its dynamics. The kinodynamic planning signal inherits the guidance capabilities of the harmonic gradient field. It can also be easily configured to efficiently suppress the inertia-induced transients in the robot's trajectory without compromising the speed of operation. The approach works with dissipative systems as well as systems acted on by external forces without needing the full knowledge of the system's dynamics. Theoretical developments and simulation results are provided in this article.

The HPF approach to planning is emerging as a powerful paradigm for the guidance of autonomous agents. Since it was suggested in the mid-late 1980s [1], [2], the approach is continuously being developed to meet the stringent requirements operation in a real-life environment imposes on an agent. Until now, the approach has amassed many attractive properties crucial for enhancing goal reachability. The approach is provably correct, driving the agent to a successful conclusion if the task is manageable and providing an indication if the task is intractable. It can be used to guide the motion of an arbitrarily shaped agent in an unknown environment regardless of its

Digital Object Identifier 10.1109/MRA.2010.935794

1070-9932/10/$26.00©2010 IEEE

The HPF approach to planning is emerging as a powerful paradigm for the guidance of autonomous agents.

geometry or topology, relying only on the sensory data acquired online by the agent's finite-range sensors. The method can also impose a variety of constraints on the agent's trajectory such as regional avoidance and directional constraints [3]–[8]. Harmonic functions are also Morse functions and a general form of the navigation functions suggested in [13] (see "Navigation Functions").

A planner may be defined as an intelligent, purposive, context-sensitive controller that can instruct an agent on how to deploy its motion actuators (i.e., generate a control signal) so that a target state may be reached in a constrained manner. Traditionally, a planning task is distributed at two stages: a high-level control (HLC) and a low-level control (LLC). The HLC stage receives data about the environment, the target of the agent, and constraints on its behavior. It then simultaneously processes these data to generate a reference plan or trajectory marking the desired behavior of the robot. This trajectory, if actualized, leads to the agent reaching its target in the specified manner. The reference trajectory is then fed to an LLC to convert it into a sequence of action instructions to be executed by the agent's actuators of motion. Unfortunately, the HLC-LLC paradigm for planning suffers from serious problems that adversely impact its performance in a realistic setting. An alternative may be achieved by fusing the HLC and LLC modules into one called the navigation control. A navigation control attempts to directly convert the environmental data, goal of the robot, and constraints on its behavior into a control signal. Khatib potential field approach may be considered as one of the first methods to cast planning in a navigation control framework [9]. The potential field approach enjoys several attractive features: most significant is the high speed by which a robot can respond to the contents of its environment.

The attractor–repeller setting that is used to generate the potential field has some problems. The most serious one has to do with convergence, where it was observed that a robot guided by such a method may stop somewhere in the workspace before reaching its target; the problem was termed the local minima problem. Many methods were proposed to generate potential fields that do not suffer from this problem [10]–[12]. Koditschek diffeomorphism approach [13] was among the first methods suggested as a remedy to this shortcoming. To convert the gradient guidance field from the potential surface ($-\nabla V$) into a control signal (u), Koditschek and Rimon suggested that the gradient guidance field can be augmented with a viscous dampening force that is linearly proportional to speed [14]:

$$u = -b \cdot \dot{x} - \nabla V(x). \tag{1}$$

According to [14], this combination will only work provided that the initial speed of the robot at each point in space ($\omega(x)$) is lower than an upper bound $S(x)$:

$$\omega(x) \leq S(x) \qquad x \in \Omega, \tag{2}$$

where Ω is the workspace of the robot. Practical application of the earlier faced two difficulties: first, no method was provided to compute the upper bound S. Even if a method is devised for doing so, there is no guarantee that, in a practical situation, the initial speed of a robot can be made to lie below the admissible upper bound. The second difficulty has to do with the fact that the satisfaction of the upper speed constraint guarantees only that obstacle avoidance constraints will be upheld and convergence to the target will be achieved. In potential field methods, transients can be a serious concern that could make it impractical to use these techniques for controlling a robot. Also, the approach seems to deal only with dissipative systems where no mention of how the method may be applied when external forces such as gravity are present.

In its current form, the HPF approach can only operate in an HLC mode providing only a guidance signal from the gradient of the potential. This signal has to be converted into a control signal by an LLC. Guldner and Utkin suggested an interesting approach based on a sliding-mode (SM) control for converting the gradient field from an HPF into a control signal [21]. The approach is robust, has good convergence properties, does not require full knowledge of system dynamics, and can make, with little transients, the dynamic trajectory of the robot follow the kinematic trajectory marked by the gradient field. The main drawback of the approach seems to be the high chattering that the control signal experiences.

It is shown that an NADF-based control can efficiently suppress inertia-induced artifacts in the dynamical trajectory of the system, making it closely follow the kinematic trajectory while maintaining an agile system response. The approach does not require the system dynamics to be fully known. A loose upper bound is sufficient for constructing a well-behaved control signal that can deal with dissipative systems as well as systems being influenced by external forces (e.g., gravity). An earlier version of this work may be found in [32].

This article is organized as follows: The "Background" provides a brief background of the potential field approach. An intuitive solution for converting a gradient guidance filed into a navigation control signal is presented in the "The NADF Approach" section. The "Dissipative Systems" and "Systems with External Forces" sections discuss the application of the approach to dissipative systems and systems experiencing external forces, respectively. Simulation results are presented in the "Results" section and the last section draws the conclusion.

Background

The HPF approach appeared shortly after the work of Khatib. Although the approach was brought to the forefront of motion planning independently and simultaneously by different researchers [16]–[20], the first work to be published on the subject was that by Sato in 1987 [1]. The HPF approach eliminates the local minima problem encountered in [9] by forcing the differential properties of the potential field to satisfy the

Navigation Functions

Definition: Let $V(x)$ be a smooth (at least twice differentiable) scalar function [$V(x)$: $R^N \rightarrow R$]. A point x_o is called a critical point of V if the gradient vanishes at that point ($\nabla V(x_o) = 0$); otherwise, x_o is regular. A critical point is Morse, if its Hessian matrix ($H(x_o)$) is nonsingular. $V(x)$ is Morse, if all of its critical points are Morse [24].

Proposition: If $V(x)$ is a harmonic function defined in an N-dimensional space (R^N) on an open set Ω, then the Hessian matrix at every critical point of V is nonsingular, i.e., V is Morse.

Proof: There are two properties of harmonic functions that are used in the proof.

1) A harmonic function ($V(x)$) defined on an open set Ω contains no maxima or minima, local or global in Ω. An extrema of $V(x)$ can only occur at the boundary of Ω.
2) If $V(x)$ is constant in any open subset of Ω, then it is constant for all Ω. Other properties of harmonic functions may be found in [26].

Let x_o be a critical point of $V(x)$ inside Ω. Since no maxima or minima of V exist inside Ω, x_o has to be a saddle point. Let $V(x)$ be represented in the neighborhood of x_o using a second-order Taylor series expansion:

$$V(x) = V(x_o) + \nabla V(x_o)^T (x - x_o) + \frac{1}{2}(x - x_o)^T H(x_o)(x - x_o) \qquad \|x - x_o\| \ll 1. \tag{A1}$$

Since x_o is a critical point of V, we have

$$V' = V(x) - V(x_o) = \frac{1}{2}(x - x_o)^T H(x_o)(x - x_o) \qquad \|x - x_o\| \ll 1. \tag{A2}$$

Note that adding or subtracting a constant from a harmonic function yields another harmonic function, i.e., V' is also harmonic. Using eigenvalue decomposition [25]:

$$V' = \frac{1}{2}(x - x_o)^T U^T \begin{bmatrix} \lambda_1 & 0 & 0 & 0 \\ 0 & \lambda_2 & . & 0 \\ . & . & . & . \\ 0 & 0 & . & \lambda_N \end{bmatrix} U(x - x_o) = \frac{1}{2}\xi^T \begin{bmatrix} \lambda_1 & 0 & 0 & 0 \\ 0 & \lambda_2 & . & 0 \\ . & . & . & . \\ 0 & 0 & . & \lambda_N \end{bmatrix} \xi = \frac{1}{2}\sum_{i=1}^{N} \lambda_i \xi_i^2, \tag{A3}$$

where U is an orthonormal matrix of eigenvectors, λs are the eigenvalues of $H(x_o)$, and $\xi = [\xi_1\ \xi_2 \ldots \xi_N]^T = U(x - x_o)$. Since V' is harmonic, it cannot be zero on any open subset Ω; otherwise, it will be zero for all Ω, which is not the case. This can only be true if and only if all the λ_i's are nonzero. In other words, the Hessian of V at a critical point x_o is nonsingular. This makes the harmonic function V also a Morse function.

Computing the Normal Component

Constructing an NADF force requires that the component of motion normal to $-\nabla V$ be computed. Explicit computation of such component requires that $N - 1$ set of basis vectors fully spanning the normal space be constructed. Although explicitly constructing such basis in R^N is possible, it is desirable that the normal component of motion be computed using an indirect approach that relies only on $-\nabla V$. This may be carried out using the following steps:

1) compute the component of motion in-phase with $-\nabla V(x_r)$

$$x_r = \dot{x}^T \frac{-\nabla V(x)}{\|\nabla V(x)\|}, \tag{A4}$$

2) remove the in-phase component from $\dot{X}$ creating the vector

$$x_n = \dot{x} - x_r \cdot \frac{-\nabla V(x)}{\|\nabla V(x)\|}, \tag{A5}$$

3) normalize $\mathbf{x}_n$ to obtain the normal vector μ:

$$\mu = \frac{x_n}{\|x_n\|}, \tag{A6}$$

4) the orthogonal component may now be computed as

$$|\dot{x}^T \mu| \mu. \tag{A7}$$

The following example demonstrates that the aforementioned process is equivalent to the direct procedure.

At a certain point in space, let $-\nabla V = [1/\sqrt{2}\ \ 1/\sqrt{2}]^T$, $\mathbf{n} = [-1/\sqrt{2}\ \ 1/\sqrt{2}]^T$, and $\dot{x} = [0.6\ \ -1]^T$. Using the direct procedure, the normal component is

$$(\dot{x}^T \mathbf{n}) \cdot \mathbf{n} = [0.2 \quad -0.2]^T. \tag{A8}$$

Using the indirect procedure, we have

$$x_r = \dot{x}^T(-\nabla V) = -0.28284, \tag{A9}$$

$$x_n = \dot{x} - x_r \cdot A(-\nabla V) = [0.8 \quad -0.8]^T, \tag{A10}$$

normalizing $\mathbf{x}_n$, we have

$$\boldsymbol{\mu} = [1/\sqrt{2} \quad -1/\sqrt{2}]^T. \tag{A11}$$

The orthogonal component of motion is

$$|\dot{x}^T \boldsymbol{\mu}| \cdot \boldsymbol{\mu} = [0.2 \quad -0.2]^T. \tag{A12}$$

The answer is the same as the one from the direct approach.

After motion is trapped by the clamping control, an iterative procedure is suggested for totally canceling the error.

Laplace equation inside the workspace of the robot (Ω) while constraining the properties of the potential at the boundary of Ω ($\Gamma = \partial\Omega$). The boundary set Γ includes both the boundaries of the forbidden zones (O) and the target point (x_T). A basic setting of the HPF approach is:

$$\nabla^2 V(x) \equiv 0 \qquad x \in \Omega,$$
$$\text{subject to: } V_i = 0|_{X=C_i} \quad \text{and} \quad V_i = 1|_{X\in\Gamma_i'}. \tag{3}$$

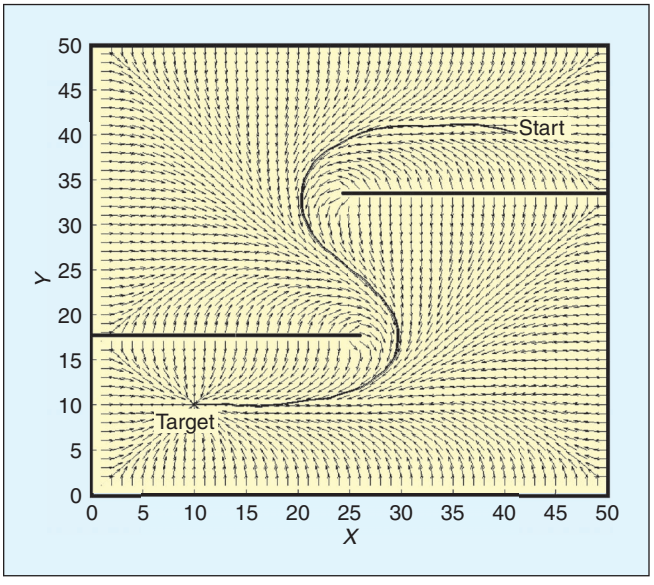

Figure 1. *Guidance field and generated trajectory of an HPF.*

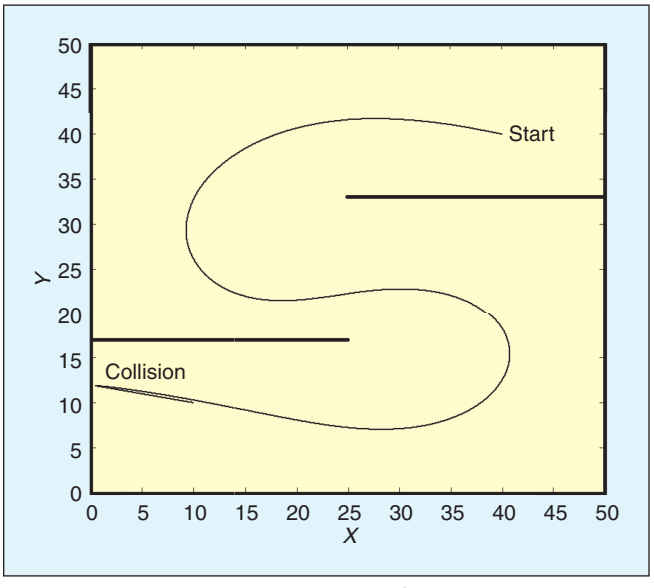

Figure 2. *Trajectory generated by the field in Figure 1.*

The trajectory to the target ($x(t)$) is generated using the HPF-based, gradient dynamical system:

$$\dot{x} = -\nabla V(x) \qquad x(0) = x_0 \in \Omega. \tag{4}$$

The trajectory is guaranteed to:

$$\lim_{t\to\infty} x(t) \to x_T x(t) \in \Omega \quad \forall t, \tag{5}$$

whereby a proof of (5) may be found in [3]. Figure 1 shows the negative gradient field of a harmonic potential and the trajectory, $x(t)$, generated using the gradient dynamical system in (4) for the simple environment of a room with two dividers. The HPF approach is only a special case of a broader class of planners called partial differential equation–ordinary differential equation (PDE-ODE) motion planners [5] where the field is generated using the boundary value problem:

$$\text{solve: } L(V(x)) \equiv 0 \qquad x \in \Omega,$$
$$\text{subject to: } \Psi(V(x)) = 0 \quad x \in \Gamma. \tag{6}$$

The trajectory is generated using the nonlinear system:

$$\dot{x} = F(V(x)) \quad x(0) = x_0 \in \Omega, \tag{7}$$

where L is scalar partial differential operator, Ψ is a governing relation restricting the potential or some of its properties at the boundary to a certain value, F is a nonlinear vector function mapping $R \to R^N$, N is the dimension of x. Planners assuming a PDE-ODE setting other than that of the one in (3) may be found in [3], [7], and [8].

The trajectory, $x(t)$, generated by the dynamical system in (4) is only a reference trajectory that should be fed to an LLC to generate the control signal u. One way of converting the guidance signal into a control signal is to augment the gradient field with a component that is proportional to speed. This seemingly straightforward solution is problematic. In Figure 2, the negative gradient of the potential in Figure 1 is used to navigate a 1-kg point mass. The system equation is

$$\begin{bmatrix} \ddot{x} \\ \ddot{y} \end{bmatrix} = -b \cdot \begin{bmatrix} \dot{x} \\ \dot{y} \end{bmatrix} - \begin{bmatrix} \partial v(x, y)/\partial x \\ \partial v(x, y)/\partial y \end{bmatrix}, \tag{8}$$

where $b = 0.1$. Despite the initial speed being zero, the trajectory violated the avoidance condition and collided with the wall.

The NADF Approach

An intuitive solution for converting a gradient guidance field into a navigation control signal is to increase the coefficient of the linear velocity term to a sufficiently high level. The linear velocity component acts as a dampener of motion that may be used to place the inertial force under control by marginalizing its disruptive influence on the trajectory of the robot that the gradient field is attempting to generate. The following example demonstrates that this solution is

impractical. To generate a control signal that would satisfy the avoidance constraints (5), the coefficient of damping of the system is increased to $b = 0.15$. The resulting trajectory and the distance to the target as a function of time are shown in Figures 3 and 4, respectively. Although the trajectory did converge to the target point (x_T) and did not violate the regional avoidance constraints, unacceptable transients along with significant deviations from the path marked by the gradient field (Figure 1) are present. In a second attempt to generate a well-behaved control signal, the dampening coefficient is significantly increased to $b = 0.7$. Although a well-behaved trajectory was obtained (Figure 5), significant slowdown of motion did occur (Figure 6).

The method for converting the gradient field from a harmonic potential into a navigation control signal by simple augmentation with a linear velocity damping term is incorrect. This approach ignores the dual role that the gradient field acts as a control and guidance provider. This field guides a robot to the target using vectors that point out the directions along which the robot has to move if the target is to be reached and the obstacles are to be avoided. At the same time, these vectors are forces that act on the mass of the robot to actuate motion. The inertia of the robot will have a disruptive influence on motion. The linear damping term manages the inertial forces in an attempt to make the motion yield to the guidance provided by the gradient field. A damping component that is proportional to velocity exercises omnidirectional attenuation of motion regardless of the direction along which it is heading. This means that the useful component of motion marked by the direction along which the goal component of the gradient of the potential is pointing is treated in the same manner as the unwanted inertia-induced component of the trajectory. These two components should not be treated equally. Attenuation should be restricted to the inertia-caused disruptive component of motion, while the component in conformity with the guidance of the artificial potential should be left unaffected (Figure 7).

To manage the effect of the inertial forces better, a damping component that treats the gradient of the artificial potential both as an actuator of dynamics and as a guiding signal is needed. A damping force (h) that behaves in the aforementioned manner is

$$h(x,\dot{x}) = \left[(\mathbf{n}^t \dot{x}\mathbf{n} + \left(\frac{\nabla V(x)^T}{\|\nabla V(x)\|} \cdot \dot{x} \cdot \Phi(\nabla V(x)^T \dot{x})\right) \frac{\nabla V(x)}{\|\nabla V(x)\|}\right], \tag{9}$$

where $\mathbf{n}$ is a unit vector orthogonal to ∇V and Φ is the unit step function. This force is given the name NADF. For the two-dimensional case, an NADF has the form:

$$h = \frac{1}{g_x^2 + g_y^2}\left[(g_x\dot{y} - g_y\dot{x}) \cdot \begin{bmatrix} -g_y \\ g_x \end{bmatrix} + (g_x\dot{x} + g_y\dot{y}) \cdot \Phi(-g_x\dot{x} - g_y\dot{y}) \begin{bmatrix} g_x \\ g_y \end{bmatrix}\right], \tag{10}$$

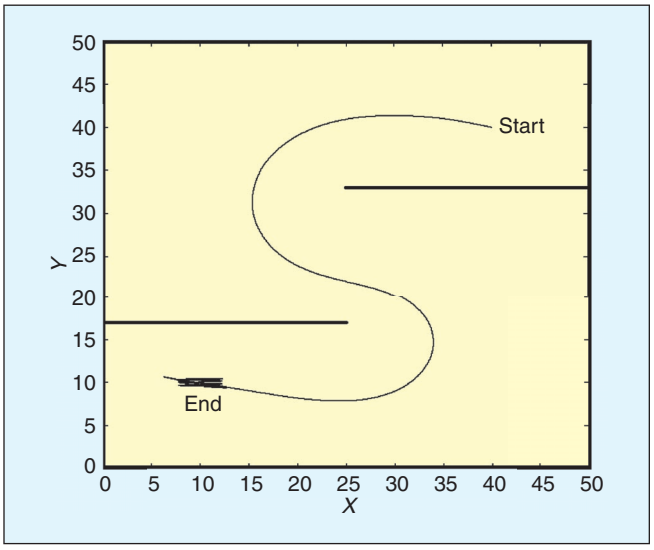

Figure 3. *Trajectory, point mass, and linear damping increased.*

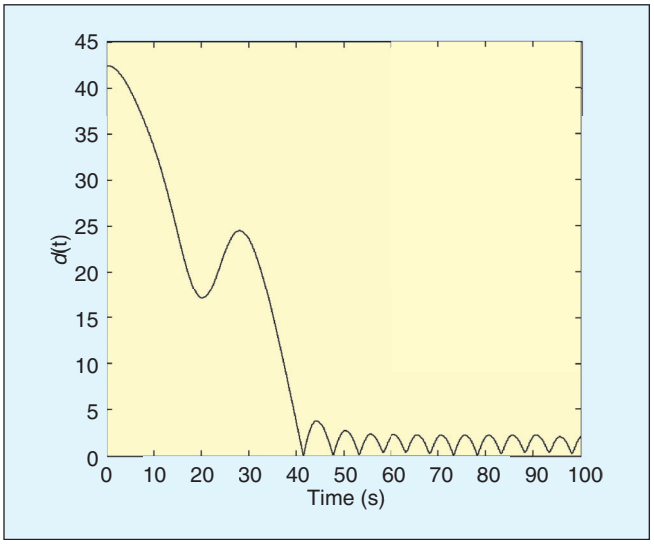

Figure 4. *Distance to target versus time ($b = 0.15$).*

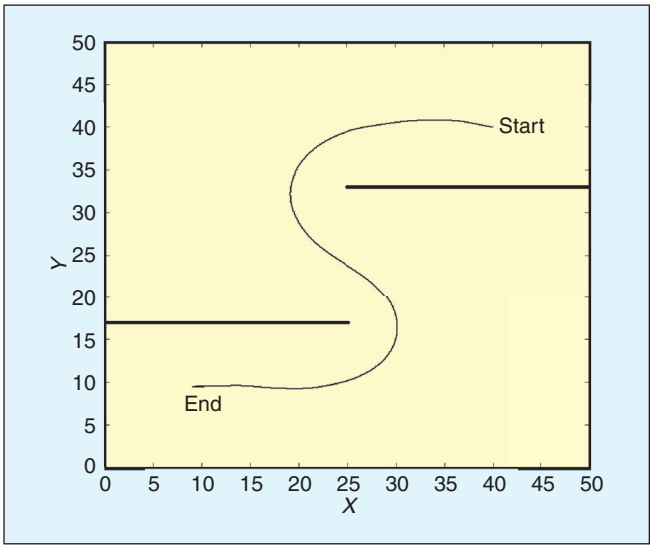

Figure 5. *Trajectory, high-linear damping.*

Different switching thresholds are used to assess the sensitivity of the procedure to the presence of transients.

where $\nabla V(x, y) = [g_x \quad g_y]^T$. A procedure for computing the component of motion normal to $-\nabla V$ in R^N is in "Computing the Normal Component."

Dissipative Systems

In this section, two propositions are stated and proven. The first proposition shows that a gradient field of a harmonic potential generated by the boundary value problem in (3) combined with NADF can guarantee global, asymptotic convergence of a fully actuated second-order dissipative dynamical system. The second shows that the dynamic trajectory of the system can be made arbitrarily close to the kinematic trajectory generated by the system in (4), hence, preserving the spatial constraints.

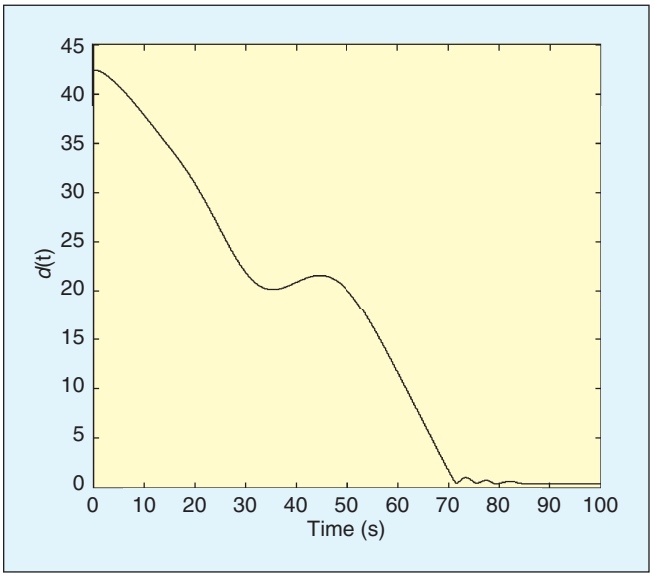

Figure 6. *Distance to target versus time (b = 0.7).*

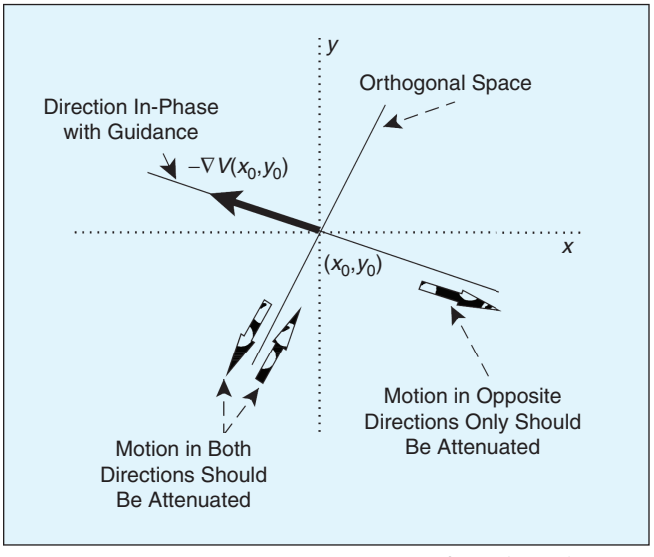

Figure 7. *Nonlinear, anisotropic, damping force (NADF).*

Proposition 1

Let $V(x)$ be a harmonic potential generated using the boundary value problem in (3). The trajectory of the dynamical system:

$$D(x)\ddot{x} + C(x, \dot{x})\dot{x} = u,$$
$$u = -b_{\mathrm{d}} \cdot h(x, \dot{x}) - k \cdot \nabla V(x), \tag{11}$$

will globally, asymptotically converge to

$$\lim_{t\to\infty} \begin{bmatrix} \mathbf{x} \\ \dot{\mathbf{x}} \end{bmatrix} \to \begin{bmatrix} \mathbf{x_T} \\ \mathbf{0} \end{bmatrix}, \tag{12}$$

for any positive constants b_{d} and k, where $\mathrm{x} \in \mathrm{R}^{\mathrm{N}}$, $\mathrm{V(x)}$: $\mathrm{R}^{\mathrm{N}} \to \mathrm{R}$, $\mathrm{D(x)}$ is an $N \times N$ positive definite inertia matrix, $C(x, \dot{x})\dot{x}$ contains the centripetal, Coriolis, and gyroscopic forces. Proof of the earlier proposition is carried out using the LaSalle principle [23].

Proof: Let Ξ be the Liapunov function candidate:

$$\Xi(x, \dot{x}) = k \cdot V(x) + \frac{1}{2}\dot{x}^T D(x)\dot{x}. \tag{13}$$

Note that as $V(x)$ is harmonic, it must assume its maxima on Γ and minima on x_T. In other words, $V(x)$ can only be zero at x_T; otherwise, its value is greater than zero:

$$\Xi(x, \dot{x}) = \begin{bmatrix} 0 & \text{if} \quad x = x_T, \dot{x} = 0 \\ \text{positive} & \text{otherwise.} \end{bmatrix} \tag{14}$$

The time derivative of the earlier function is

$$\dot{\Xi}(x, \dot{x}) = k \cdot \nabla V(x)^T \dot{x} + \frac{1}{2}\dot{x}^T \dot{D}(x)\dot{x} + \dot{x}^T D(x)\ddot{x}. \tag{15}$$

Substituting

$$\ddot{x} = D^{-1}(x)[-C(x, \dot{x})\dot{x} - b_{\mathrm{d}} \cdot h(x, \dot{x}) - k \cdot \nabla V(x)], \tag{16}$$

along with (9) in the earlier equation yields

$$\begin{aligned} \dot{\Xi} = {} & k \cdot \nabla V(x)^T \dot{x} + \frac{1}{2}\dot{x}^T \dot{D}(x)\dot{x} \\ & -k \cdot \nabla V(x)^T \dot{x} - \dot{x}^T C(x, \dot{x})\dot{x} \\ & -b_{\mathrm{d}} \cdot \dot{x}^T (n^T \dot{x})\mathbf{n} \\ & -b_{\mathrm{d}} \cdot \dot{x}^T \left(\frac{\nabla V(x)^T}{|\nabla V(x)|} \cdot \dot{x} \cdot \Phi(-\nabla V(x)^T \dot{x}) \right) \frac{\nabla V(x)}{|\nabla V(x)|}. \end{aligned} \tag{17}$$

Using the passivity property:

$$\dot{x}^T (\dot{D}(x) - 2 \cdot C(x, \dot{x}))\dot{x} = 0, \tag{18}$$

and rearranging the terms, we get

$$\dot{\Xi} = -b_{\mathrm{d}} \cdot (\mathbf{n}^T \dot{x})^T (\mathbf{n}^T \dot{x}) - b_{\mathrm{d}} \cdot \frac{(\nabla V(x)^T \cdot \dot{x})^T}{|\nabla V(x)|} \cdot \frac{(\nabla V(x)^T \cdot \dot{x})}{|\nabla V(x)|} \cdot \Phi(\nabla V(x)^T \dot{x}), \quad (19)$$

as can be seen

$$\dot{\Xi} \leq 0 \qquad \forall\, x, \dot{x}, \quad (20)$$

where

$$\dot{\Xi} = 0 \qquad \text{for} \quad \forall x \in \Omega, \dot{x} = 0,$$

according to LaSalle principle any bounded solution of (11) will converge to the minimum invariant set:

$$E \subset \{\dot{x} = 0, x\}. \quad (21)$$

Determining E requires studying the critical points of $V(x)$. According to the maximum principle, x_T is the only minimum (stable equilibrium point) $V(x)$ can have. Besides x_T, $V(x)$ has a finite number of isolated critical points $\{x_i\}$ at which $\nabla V = 0$; however, the Hessian at these points is nonsingular, i.e., $V(x)$ is Morse [24]. A proof of this result may be found in "Navigation Functions." It is concluded that E contains only one point, $x = x_T, \dot{x} = 0$, to which motion will converge. A proof based on Liapunov theory showing that, for the kinematic case, $-\nabla V(x)$ can drive motion from anywhere in Ω to x_T may be found in [3].

Proposition 2

Let ρ be the trajectory constructed as the spatial projection of the solution, $x(t)$, of the first-order differential system in (4). Also, let ρ_{d} be the trajectory constructed as the spatial projection of the solution, $x(t)$, of the second-order system in (11) (Figure 8). Then there exist a b_{d} that can make the maximum deviation (δ_{m}) between ρ and ρ_{d} arbitrarily small.

Proof: The gradient field from an HPF does not only work as a guide of motion to the target but also be used to cover Ω with a complete set of boundary-fitted basis [4] coordinates.

The radial basis of the system ($\Delta V/|\Delta V|$) marks the useful component of motion. The basis orthogonal to this component spans the instantaneous deviation between ρ and $\rho_{\mathrm{d}}(\delta)$, which NADF is required to attenuate (Figure 9).

The dynamic equation describing the disruptive component is

$$\mathbf{n^T} D(x)\ddot{x} + \mathbf{n^T} C(x, \dot{x})\dot{x} + b_{\mathrm{d}} \cdot \mathbf{n^T} h(x, \dot{x}) + k \cdot \mathbf{n^T} \nabla V(x) = 0. \quad (22)$$

Examining the earlier equation term by term yields

1) $$\mathbf{n}^T \nabla V = 0, \quad (23)$$

2) $$\mathbf{n^T}\left[(\mathbf{n}^t \dot{x})n + \left(\frac{\nabla V(x)^T}{|\nabla V(x)^T|} \cdot \dot{x} \cdot \Phi(\nabla V(x)^T \dot{x})\right), \frac{\nabla V(x)}{|\nabla V(x)|}\right] = (\mathbf{n}^t \dot{x})$$

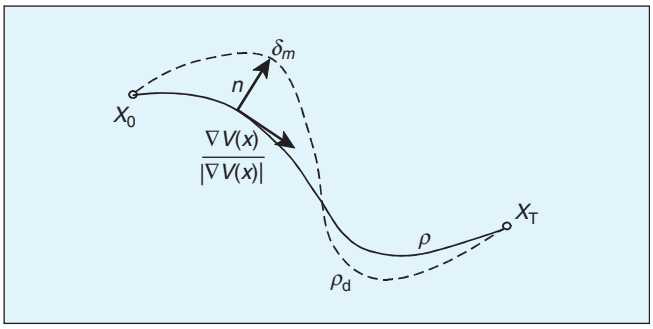

Figure 8. *The kinematic and dynamic trajectories.*

3) assuming a stable and nonimpulsive system, an upper bound can be placed on the speed:

$$|\dot{x}| \leq v_{\max}, \quad (24)$$

Therefore, the norm of the matrix C may be bound as:

$$\|\mathbf{C}(x, \dot{x})\| \leq c_{\max}, \quad (25)$$

4) any inertia matrix belonging to a physical system is positive definite, invertible, and have a bounded norm:

$$\|D(x)\| \leq d_{\max}, \quad (26)$$

where $d_{\max}$, $c_{\max}$, and $v_{\max}$ are finite, positive constants. A dynamic equation that yields an upper bound on δ is

$$d_{\max} \cdot \mathbf{n}^T \ddot{x} - c_{\max} \mathbf{n}^T \dot{x} + b_{\mathrm{d}} \cdot \mathbf{n}^T \dot{x} = 0, \quad (27)$$

or

$$\ddot{\delta} + \Delta \cdot \dot{\delta} = 0,$$

where

$$\ddot{\delta} = \mathbf{n}^T \ddot{x}, \dot{\delta} = n^{\mathbf{T}} \dot{\mathbf{x}}, \quad \text{and} \quad \Delta = \frac{b_{\mathrm{d}} - c_{\max}}{d_{\max}}.$$

To determine the effect of the disruptive time component ($\xi(t)$) that acts normal to ∇V, the impulse response ($z(t)$) of (27) is obtained:

$$z(t) = \frac{1}{\Delta}(1 - \mathbf{e}^{-\Delta \cdot \mathbf{t}})\Phi(\mathbf{t}) = \frac{z(t)}{\Delta}. \quad (28)$$

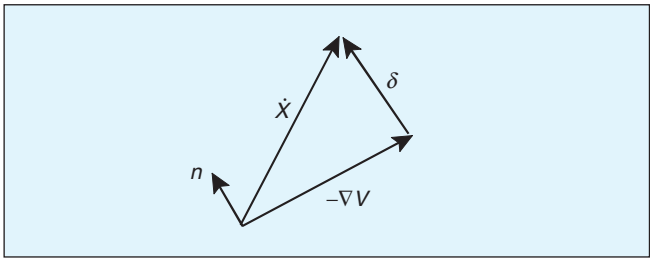

Figure 9. *The disruptive component of motion.*

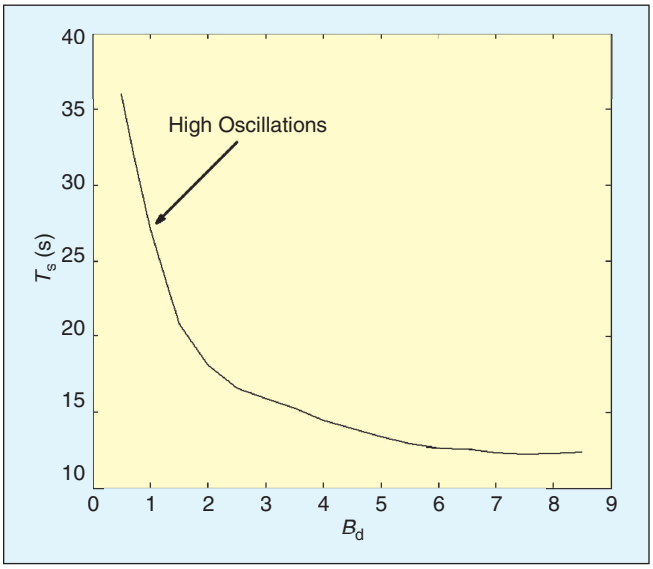

Figure 10. *Settling time versus NADF coefficient.*

The deviation as a function of time may be computed as

$$\delta(\mathbf{t}) = \xi(\mathbf{t}) * z(t),$$

where * denotes the convolution operation. As shown in Proposition 1 that motion will converge to x_T and all dynamic terms will tend to zero, $\xi(t)$ may be bounded as

$$\int_0^\infty |\xi(t)|dt \leq I, \tag{29}$$

therefore

$$\delta(t) = \frac{\mathbf{1}}{\Delta} z(t) * \xi(t) \leq \frac{I_{\max}}{\Delta},$$

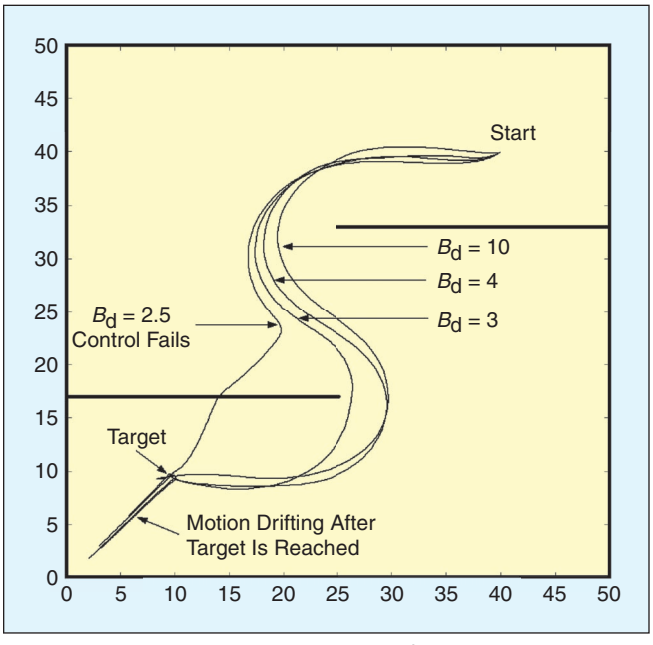

Figure 11. *Trajectory, NADF—external force present.*

where I and $I_{\max}$ are positive constants. By properly selecting a value for Δ, the maximum deviation δ_m can be made arbitrarily small. In other words, the dynamic trajectory of (11) will closely follow the kinematic trajectory of (4), and the spatial constraints will be preserved. Since NADF is by design made to be zero when motion is in accordance with the guidance field ∇V, b_d can be made arbitrarily large without slowing down the system. This fact is clearly reflected by the simulation results (Figure 10).

Systems with External Forces

The NADF approach may be adapted for designing constrained motion controller for mechanical systems experiencing external forces (e.g., gravity). The dynamical equation of such systems has the form

$$D(x)\ddot{x} + C(x, \dot{x})\dot{x} + g(x) = F, \tag{30}$$

where $g(x)$ and F are vectors containing the external forces and the applied control forces, respectively. A controller consisting of the gradient guidance field and a strong enough NADF (31) has the ability to make the trajectory of the system in (30) closely follow the kinematic trajectory from an initial starting point (x_o) to the target point x_T,

$$F = -b_d \cdot h(x, \dot{x}) - k \cdot \nabla V(x). \tag{31}$$

However, because of the presence of the external forces, the controller will not be able to hold the state close to the target point and drift will occur (Figure 11). Arimoto and Miyazaki showed that steady-state error caused by the external forces may be canceled by using an integral control action [27]. Unfortunately, an integral action raises the order of the mechanical system and could cause it to become unstable if it is not tuned properly. The integrator also induces a difficult to manage transients in the system response.

Here an alternative approach to using an integrator is suggested. The suggested approach does not endanger stability and can cancel the error caused by the external forces bringing the dynamic trajectory arbitrarily close to the target point. The approach capitulates on the ability of the controller in (31) to drive motion arbitrarily close to the target point. Once the trajectory is close to the target, a passive clamping control action is activated to trap the trajectory in a set close to the target. After motion is trapped by the clamping control, an iterative procedure is suggested for totally canceling the error. In the following, the suggested clamping control is described.

Clamping Control

The effect of the clamping control (F_c) is strictly localized to a hypersphere of constant radius σ surrounding the target point. If motion is heading toward the target, this control component is inactive. On the other hand, if motion starts heading away from the target, the control becomes active and attempts to drive the trajectory back to the target (Figure 12).

A clamping control that behaves in the earlier manner is:

$$F_C(x, \dot{x}) = (x - x_T) \cdot \Phi(\sigma - |x - x_T|) \cdot \Phi(\dot{x}^T(x - x_T)). \tag{32}$$

The strength of F_c is adjusted by multiplying it with a constant k_c, so that the steady-state error is kept below a desired level (ε). Unlike the integrator, the use of a clamping control will keep the mechanical system stable for any positive value of k_c.

Proposition 3

For the mechanical system in (30), a controller of the form

$$F = -b_d \cdot h(x, \dot{x}) - k \cdot \nabla V(x) - k_C \cdot F_C(\dot{x}, x), \tag{33}$$

can make

$$\lim_{t\to\infty} |x(t) - x_T| \le \varepsilon < \sigma,$$

and

$$\lim_{t\to\infty} \dot{x} = 0, \tag{34}$$

provided that:

1) k, b_d, and k_c are all positive,
2) $$k_c \ge F_{max}/\varepsilon$$
$$F_{max} = \max_x |g(x)| \quad x \in \Omega_\sigma,$$
and
$$\Omega_\sigma = \{x : |x - x_T| \le \sigma\}, \tag{35}$$
3) a high enough value of b_d is selected so that at some instant in time t'
$$|x(t') - x_T| < \sigma, \tag{36}$$
4) k is high enough so that the gradient field is capable of directing the trajectory to Ω_σ
$$|k \cdot \nabla V(x)| > \left| g^T(x) \frac{\nabla V(x)}{|\nabla V(x)|} \right| \quad x \in \Omega - \Omega_\sigma. \tag{37}$$

Proof: Consider a Liapunov function candidate similar to the one in (13) with a gravitational potential energy term ($P(x)$) added:

$$\Xi(x, \dot{x}) = k \cdot V(x) + \frac{1}{2}\dot{x}^T D(x)\dot{x} + P(x), \tag{38}$$

note that:

$$g(x) = -\nabla P(x) \text{ and } P(x) = \int_{\mathbf{x_0}}^{\mathbf{x}} g(z)dz. \tag{39}$$

Differentiating (38) with respect to time, we get:

$$\dot{\Xi}(x, \dot{x}) = k \cdot \nabla V(x)^T \dot{x} + \frac{1}{2}\dot{x}^T \dot{D}(x)\dot{x} + \dot{x}^T D(x)\ddot{x} + \dot{x}^T g(x), \tag{40}$$

solving for $\ddot{x}$ from (30) and (31) and substituting the results in (40) we get:

$$\begin{aligned}\dot{\Xi} = &-b_d \cdot (\mathbf{n}^T\dot{x})^T(\mathbf{n}^T\dot{x}) \\ &-b_d \cdot \frac{(\nabla V(x)^T \cdot \dot{x})^T}{|\nabla V(x)|} \cdot \frac{(\nabla V(x)^T \cdot \dot{x})}{|\nabla V(x)|} \cdot \Phi(\nabla V(x)^T\dot{x}) \\ &-k_C \cdot \dot{x}^T(x - x_T) \cdot \Phi(\dot{x}^T(x - x_T)) \cdot \Phi(\sigma - |x - x_T|).\end{aligned} \tag{41}$$

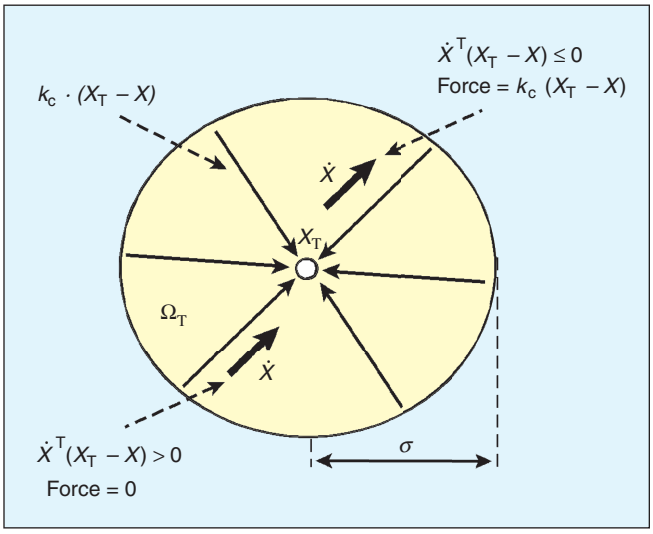

Figure 12. *The clamping control.*

As k_c and b_d are positive we have:

$$\begin{aligned}\dot{\Xi} &\le 0 \qquad \forall x, \dot{x}, \quad \text{where} \\ \dot{\Xi} &= 0 \qquad \text{for} \quad \forall x, \dot{x} = 0.\end{aligned} \tag{42}$$

Since we are assuming that k and b_d are selected high enough so that the dynamic trajectory will follow the kinematic trajectory and enter Ω_σ, the minimum invariant set to which the trajectory is going to converge may be computed from:

$$g(x) + k \cdot \nabla V(x) + k_C \cdot F_C(x, \dot{x} = 0) = 0. \tag{43}$$

Since $\Phi(0) = 1$, and $x \in \Omega_\sigma$ [i.e., $\Phi(\sigma - |x - x_T|) = 1$), (43) becomes:

$$g(x) + k \cdot \nabla V(x) + k_C \cdot (x - x_T) = 0. \tag{44}$$

If condition 2 on k_C is satisfied, the solution of the earlier equation has to lie in the set $\Omega_\varepsilon = \{x : |x - x_T| < \varepsilon\}$. This means that the deviation of the end of the dynamic trajectory from the target point should at most be ε.

Another alternative to the use of integration is to reduce steady-state error by increasing the gain of the gradient field (k) to a sufficiently high level. This approach makes the transient difficult to manage and increases the control effort. On the other hand, selecting a high gain of the clamping control (k_C) to manage the steady-state error will not cause the earlier problems. This is because this control component is designed to be minimally intrusive affecting the system only when it is needed. This is clearly demonstrated by simulation (Figures 13 and 14).

Iterative, Blind-Error Cancelation

Although clamping control has the ability to reduce the steady-state error to an arbitrarily small value, sometimes it is desired that this error be totally canceled. Here, an iterative, blind procedure is suggested for error cancelation. The procedure works by providing an alternative path (β) other than the error channel ($K_P \cdot e$, where K_P is a positive definite matrix) to

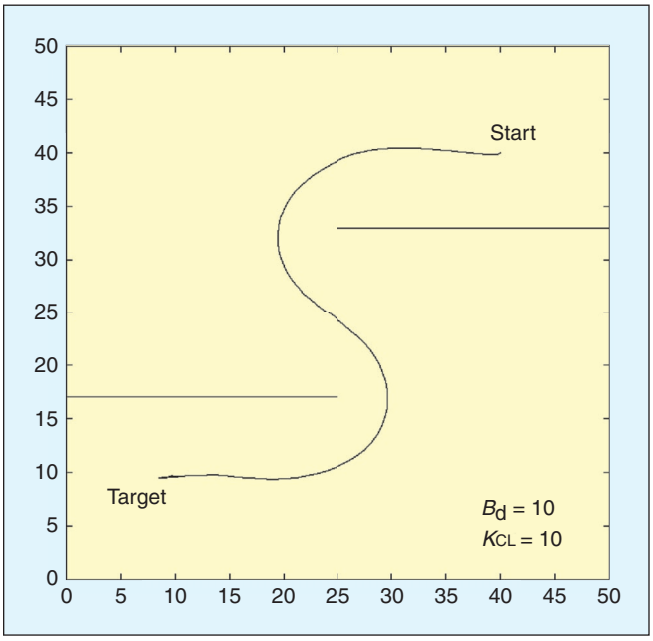

Figure 13. *Trajectory, NADF, and clamping.*

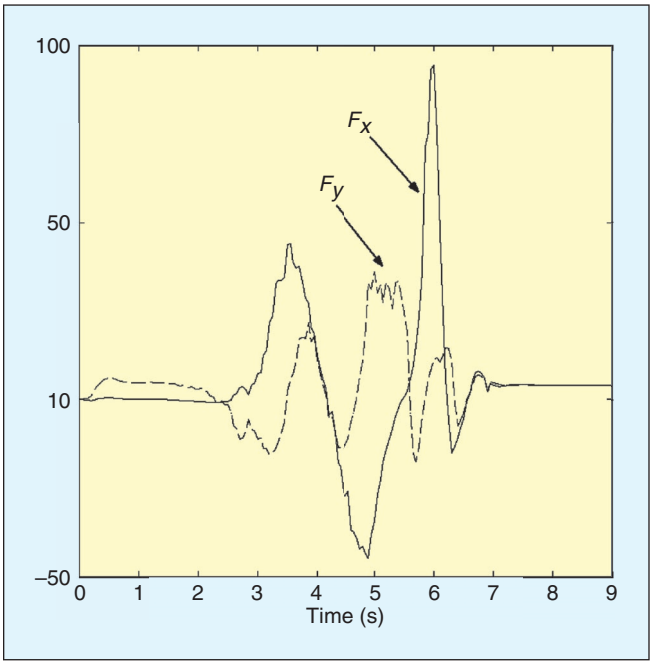

Figure 14. *x and y control force components—external force present.*

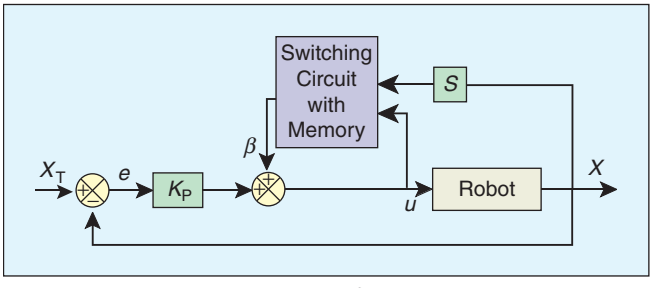

Figure 15. *The suggested scheme for iterative-error cancelation.*

supply the control signal (u) that is needed to hold the robot at a location x_T (Figure 15),

$$u = K_P \cdot e + \beta. \tag{45}$$

The fixed-point iteration method [28] is used to evolve an estimate of the control signal so that the steady-state error is driven to zero. This procedure is implemented using a switched logic circuit with one memory-storage element. One implementation requires the circuit to have two inputs: the control that is directly fed to the robot and velocity of the robot's coordinates to assess convergence (other means to decide if the robot has converged may be used). There is only one output consisting of the bias term β. The bias term is iteratively determined as follows: when motion is about to settle (i.e., $|dx/dt| < \alpha$, where $0 < \alpha \ll 1$), the circuit measures the value of u and assigns it to β. This value is kept until the event becomes true again at another instant i. At the ith instant we have

$$u = g(x_i), \beta = g(x_{i-1}), \text{ and } K_P \cdot e = K_P \cdot (x_T - x_i), \tag{46}$$

where x_i is the position of the robot at the ith settling instant. Relating the earlier quantities using (45) yields the recursive relation:

$$g(x_i) = g(x_{i-1}) + K_P \cdot (x_T - x_i). \tag{47}$$

Proposition 4

The recursive relation in (47) has a fixed point at which

$$(x_T - x_i) = 0. \tag{48}$$

Proof: Using Taylor series expansion around x_T, we have:

$$g(x) = g(x_T) + J(g(x_T))(x - x_T) + \cdots = g(x_T) + F(x - x_T), \tag{49}$$

where J is the Jacobian matrix of g and F is a function containing the $(x - x_T)$ terms of the Taylor series. Substituting (49) into (47) we get:

$$F(e_i') = F(e_{i-1}') - K_P \cdot e_i', \tag{50}$$

where

$$e_i' = -(x_T - x_i). \tag{51}$$

Now, let $\eta = F(e')$ and Q be the inverse function of F in the neighborhood of x_T. Substituting Q in (50), we obtain the recursive relation:

$$K_P \cdot Q(\eta_i) + \eta_i = \eta_{i-1}. \tag{52}$$

At a fixed point, we have: $\eta_i = \eta_{i-1}$, or

$$K_P \cdot Q(\eta_i) = 0. \tag{53}$$

Since K_P is positive definite, i.e., it is not singular:

$$Q(\eta_i) = e_i' = (x_i - x_T) = 0. \tag{54}$$

In other words: $x_i = x_T$.

Proposition 5

For any positive definite K_P, the fixed point $x = x_T$ is a stable attractor, i.e., if x_i is sufficiently close to x_T,

$$\lim_{i\to\infty} x_i \to x_T. \tag{55}$$

Proof: In the close neighborhood of x_T, (47) may be written as:

$$J(g(x_T)) \cdot (x_i - x_T) = J(g(x_T)) \cdot (x_{i-1} - x_T) + K_P \cdot (x_T - x_i). \tag{56}$$

Notice that:

$$J(g(x_T)) = J(\nabla P(x_T)) = H(x_T), \tag{57}$$

where H is the symmetric Hessian matrix. Substituting (57) in (56) yields the equation:

$$[K_P + H(x_T)] \cdot e_i = H(x_T) \cdot e_{i-1}, \tag{58}$$

where $e_i = (x_T - x_i)$.

Since K_P is positive definite and H is symmetric, they are simultaneously diagonalizable into:

$$K_P = UU^T \text{ and } H = U\Lambda U^T, \tag{59}$$

where U is a nonsingular matrix, and Λ is a diagonal matrix with nonnegative elements λ_l, $l = 1, \ldots, N$, see [29, p.86]. Using the earlier decomposition, (58) may be written as:

$$U(I + \Lambda)U^T \cdot e_i = U\Lambda U^T \cdot e_{i-1}. \tag{60}$$

Using the transformation $q_i = U^T \cdot e_i$, we have

$$q_i = A \cdot q_{i-1}, \tag{61}$$

where

$$\mathbf{A} = (\mathbf{I} + \Lambda)^{-1}\Lambda = \begin{bmatrix} \frac{\lambda_1}{1+\lambda_1} & \mathbf{0} & \cdot & \mathbf{0} \\ \mathbf{0} & \frac{\lambda_2}{1+\lambda_2} & \cdot & \mathbf{0} \\ \cdot & \cdot & \cdot & \cdot \\ \mathbf{0} & \mathbf{0} & \cdot & \frac{\lambda_N}{1+\lambda_N} \end{bmatrix}. \tag{62}$$

It is well known that the solution of (61) is

$$q_i = A^i \cdot q_0. \tag{63}$$

Since

$$0 \le \frac{\lambda_l}{1+\lambda_l} < 1 \quad l = 1, \ldots, N, \tag{64}$$

we have:

$$\lim_{i\to\infty} q_i = \lim_{i\to\infty} U^T \cdot e_i \to 0. \tag{65}$$

Since U is a nonsingular matrix,

$$\lim_{i\to\infty} e_i \to 0, \tag{66}$$

The use of the NADF approach extends beyond a single-dynamical agent.

or

$$\lim_{i\to\infty} x_i \to x_T. \tag{67}$$

Results

Point Mass in a Cluttered Environment

The gradient field in Figure 1 is augmented with NADF instead of the linear, viscous, damping forces. The combination of both gradient field and NADF is used to steer a 1-kg mass from a start point to a target point. An excessively high-damping coefficient, $b_d = 10$, is used. The trajectory of the mass is shown in Figure 16. The kinodynamic trajectory of the mass is almost identical with that marked by the gradient field (kinematics only) in Figure 1. Moreover, motion of the mass is almost six times faster than its viscous damping counterpart shown in Figure 5 with a settling time (T_S) of about 12 s compared with 72 s. Figure 17 shows the control signal (X–Y force components).

Settling Time—A Comparison

NADF and linear damping exhibit different behavior as far as convergence is considered. The settling time for the point mass with no constraints on speed example is drawn in Figure 18 as a function of the linear viscous friction coefficient (b). The T_S–b relation is convex with one value for b corresponding to a global minimum of T_S. This is expected because, for low b, high oscillations will prevent motion from quickly settling in the 5% zone around the target. On the other hand, a high value for b reduces the oscillations by slowing down the response, delaying the entrance to the 5% zone.

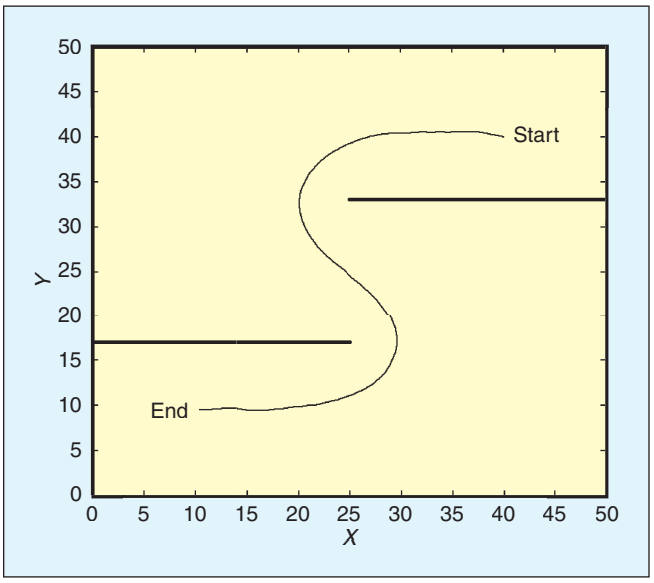

Figure 16. *Trajectory, NADF, and* $b_d = 10$.

The NADF approach may be adapted to work with second-order systems experiencing external forces using the suggested clamping control.

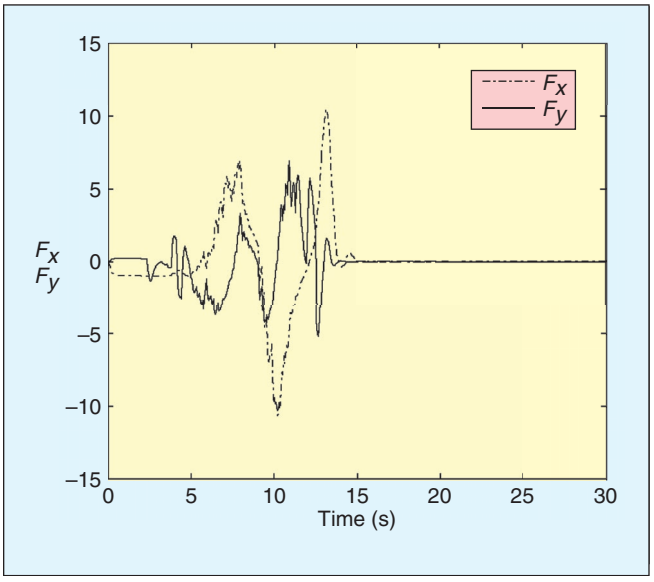

Figure 17. *x and y control force components.*

The relation between T_S and the coefficient of NADF (b_d) is a rapidly and strictly decreasing one (Figure 10). Similar to the linear case, for a low value of b_d, high oscillations will prevent the quick capture of the trajectory in the 5% zone around the target. As the value of b_d increases, NADF only impedes the component of motion along the coordinate field tangent to the gradient guidance field. This component does not contribute to convergence and only causes delay in reaching the target. Since NADF attenuates, only this component of motion leaving the motion along the gradient field unaffected, the delay in reaching the target drops as b_d increases, yielding a strictly decreasing profile of the T_S–b_d curve. The T_S versus the coefficient of damping profile is important. It determines the ability to tune the controller so that the specifications are met. In tuning the controller, there are two requirements: it is required that the maximum spatial deviation (δ_m) between the kinematic and the dynamic paths be as small as possible so that the constraints are upheld. It is also required that the settling time be as small as possible. The first requirement is achieved by making the coefficient of damping high. In the linear viscous damping case, one can only strike a compromise between T_S and δ_m. For the NADF case, this compromise is not needed, since both T_S and δ_m are strictly decreasing as a function of b_d.

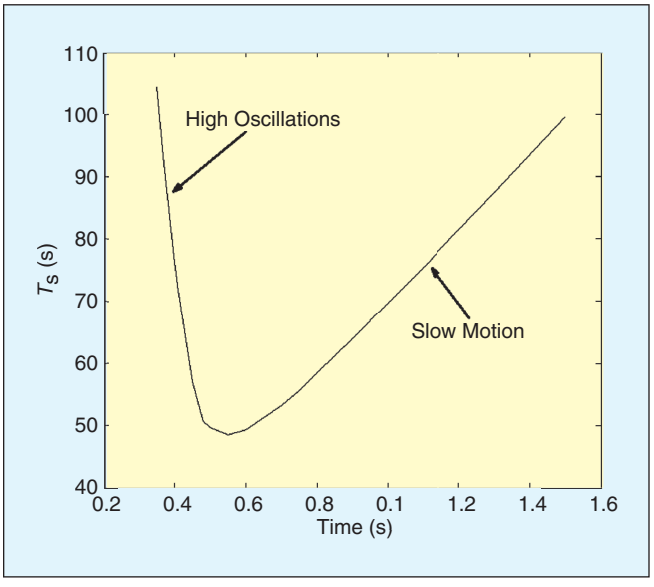

Figure 18. *T_S versus b for linear damping.*

Point Mass with External Forces

The NADF approach may be adapted to work with second-order systems experiencing external forces using the suggested clamping control. In this example, a point mass with constant external forces acting on it having the system equation in (68) is controlled using a gradient field and NADF.

$$\begin{bmatrix} \ddot{x} \\ \ddot{y} \end{bmatrix} + \begin{bmatrix} 4 \\ 4 \end{bmatrix} = \begin{bmatrix} Fx \\ Fy \end{bmatrix}. \tag{68}$$

For a sufficiently high b_d, the controller will succeed in driving the mass to the target and avoid the obstacles (Figure 11). However, when the target is reached, drift caused by the external forces occur.

In Figure 13, a clamping control similar to the one in (32) is added with $k = 1$, $b_d = 10$, and $k_C = 10$. The controller was able to hold the trajectory near the target point relying only on a loose, upper bound estimate of the drift. Despite the high value of k_C, the trajectory settled in an overdamped manner. The F_x and F_y control forces are shown in Figure 14.

The SM control approach suggested by Guldner and Utkin in [21] for converting a gradient guidance signal into a control signal has the ability to handle systems with external forces. In this approach, a sliding surface (γ) is defined as:

$$\gamma = \dot{x} - v_d(t)\frac{-\nabla V}{\|\nabla V\|}. \tag{69}$$

The control signal is

$$F = -F_0\frac{\gamma}{\|\gamma\|}, \tag{70}$$

where v_d and F_o are the maximum allowable speed and control forces, respectively. The SM control is applied to the point mass with drift in (68). The parameters of the sliding surface are set so that a settling time of 6 s is obtained. F_o is set to obtain a maximum control effort of 100 N. The trajectory is shown in Figure 19, and the control forces are shown in Figures 20 and 21.

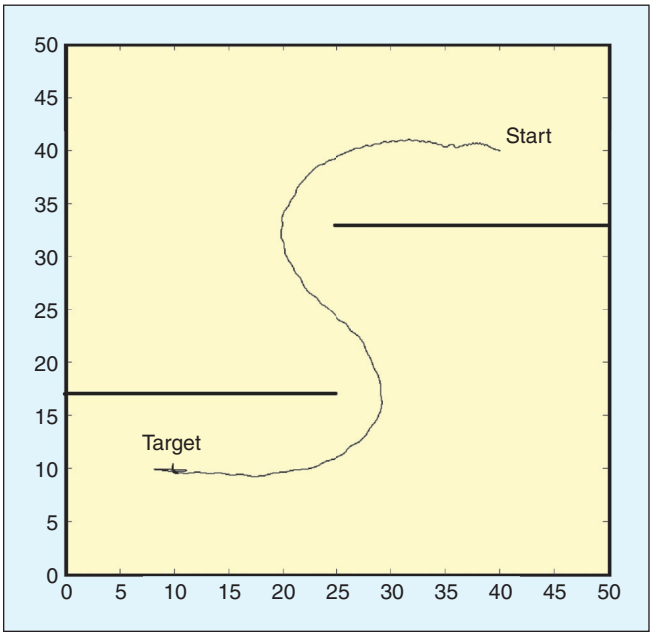

Figure 19. *Trajectory–sliding mode control.*

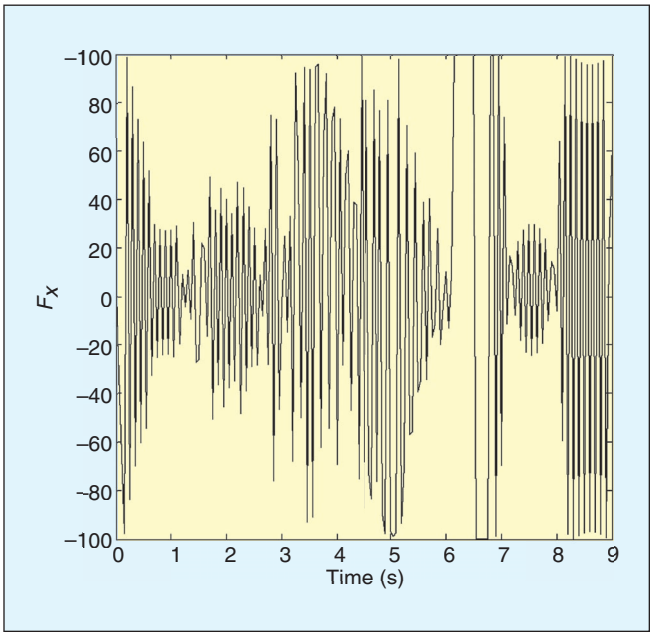

Figure 21. *x force control component.*

Compared with the NADF approach, clamping the trajectory obtained using the SM approach is a little shaky and experiences some oscillations near the target. However, the biggest difference has to do with the quality and magnitude of the control signals used by both approaches.

Iterative Error Removal

The iterative procedure to remove the steady-state error suggested in the previous section is tested using a simple pendulum with concentrated mass $m = 1$ kg and length $L = 1$ m. The dynamic equation of the pendulum is

$$m \cdot L \cdot \ddot{\Theta} + m \cdot \mathbf{g} \cdot \sin(\Theta) = u, \tag{71}$$

where g is the acceleration constant and u is the external applied control torque. A simple controller with position and velocity feedback (72) is used to move the pendulum from $\Theta = 0$ to $\Theta = \pi/2$.

$$u = -k \cdot \Theta - b \cdot \dot{\Theta}. \tag{72}$$

The weight of the pendulum causes significant steady-state error (Figure 22). To remove the error, the switching circuit suggested in V.2 is added to the controller. Different switching thresholds are used to assess the sensitivity of the procedure to the presence of transients (Figure 23). The error was eliminated in all cases. Although the iterative error cancelation procedure was designed to be used when transients fade away

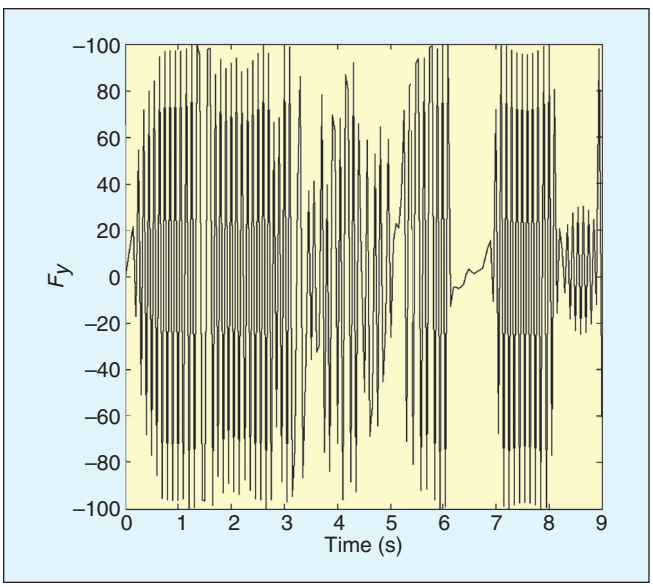

Figure 20. *y force control component.*

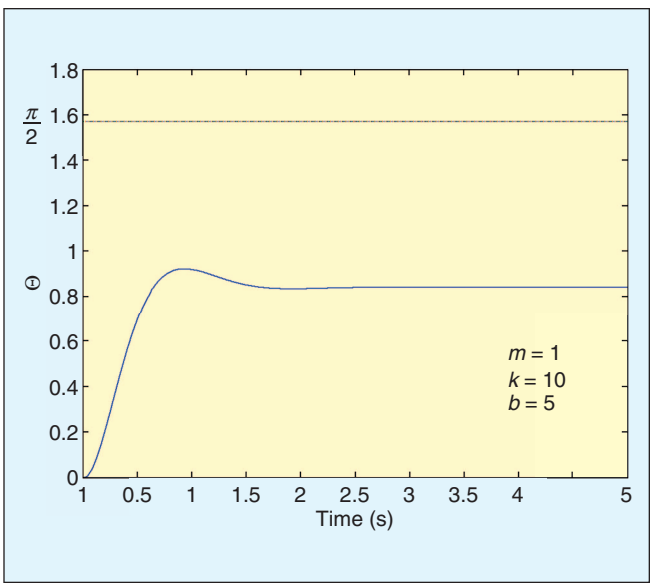

Figure 22. *Steady-state error caused by weight of pendulum.*

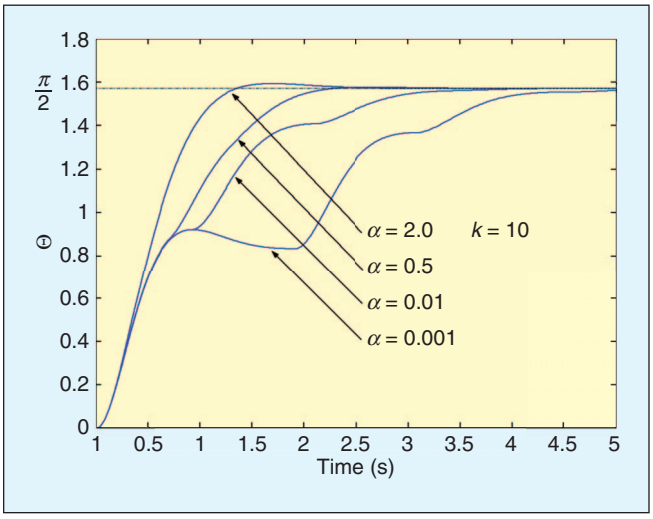

Figure 23. *Error cancelation using switching circuit—different thresholds.*

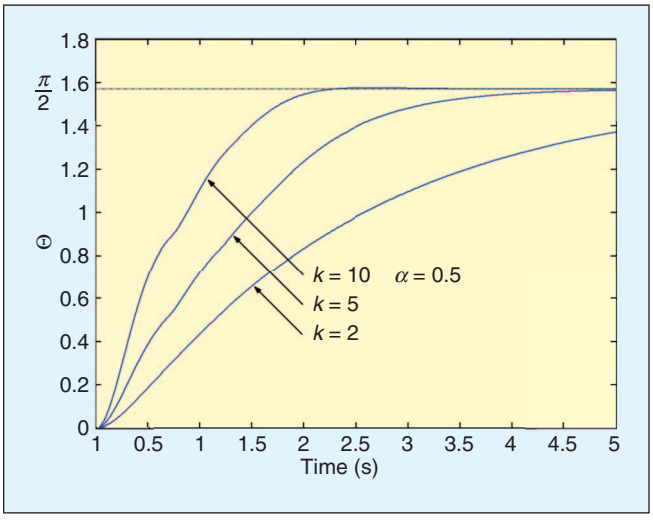

Figure 24. *Effect of forward gain on convergence.*

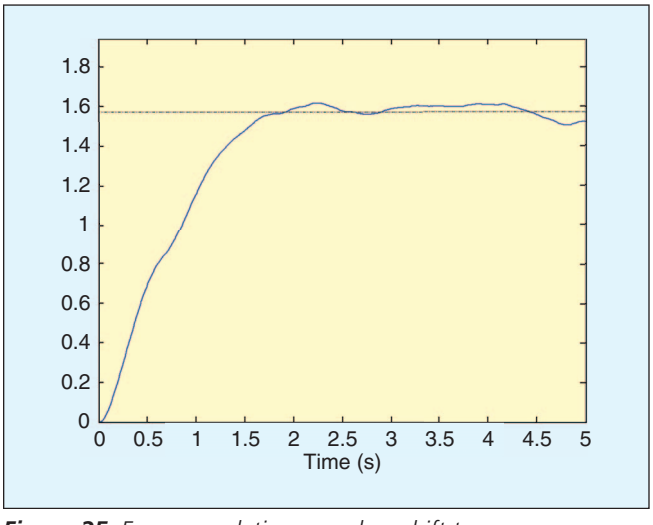

Figure 25. *Error cancelation—random drift term.*

and motion settles, simulation shows that the procedure exhibits little sensitivity to the presence of transients that enables us to loosely choose the threshold α. Actually, the simulation reveals that better results in terms of having a lower settling time could be obtained if switching is carried out before motion completely settles. In Figure 24, the effect of the forward gain on the speed of convergence is shown. As expected, the higher the forward gain the faster the system converges to its target.

If the drift term cannot be represented as the gradient of a scalar function, the iterative procedure may still work. In (73), a random drift term, χ, is added to the system equation of the pendulum:

$$m \cdot L \cdot \ddot{\Theta} + \mathbf{g} \cdot \sin(\Theta) + 10 + 10 * \chi = u, \qquad (73)$$

where χ is white noise uniformly distributed between -0.5 and 0.5. The iterative procedure is used with no modification to cancel this type of drift. The procedure was able to converge in a statistical sense to the reference (Figure 25).

The iterative blind, error cancelation procedure was also simulated for a two-link, three degrees-of-freedom arm robot manipulator. The procedure was able to effectively remove the error in a few iterations.

Conclusions

In this article, the capabilities of the HPF approach are extended to tackle the kinodynamic planning case. The extension is provably correct and bypasses many of the problems encountered by previous approaches. It is based on a novel type of nonlinear, passive damping forces called NADFs. The suggested approach enjoys several attractive properties. It is easy to tune, can generate a well-behaved control signal, the approach is flexible and may be applied in a variety of situations, and it is provably-correct. It is resistant to sensor noise, does not require exact knowledge of system dynamics, and can tackle dissipative systems as well as systems under the influence of external forces. The use of the NADF approach extends beyond a single-dynamical agent. It can be adapted for use with a multirobot dynamical system [30] as well as robots with nonholonomic constrains [31]. Most of the problems attributed to the potential field approach, namely the narrow corridor effect, are a result of the misunderstanding of the dual role a potential field plays as a motion actuator and a guidance provider [33]. The NADF approach is a step forward in taking both of these roles into account.

Acknowledgments

The author thanks Dr. Tareq AL-Naffouri for his help in proving Proposition 5 and KFUPM for its support.

Keywords

Motion, planning, harmonic, potential, navigation, control.

References

[1] K. Sato, "Collision avoidance in multi-dimensional space using laplace potential," in *Proc. 15th Conf. Robotics Society Japan*, 1987, pp. 155–156.

[2] K. Sato, "Deadlock-free motion planning using the laplace potential field," *Adv. Robot.*, vol. 7, no. 5, pp. 449–461, 1993.
[3] S. Masoud and A. Masoud, "Motion planning in the presence of directional and obstacle avoidance constraints using nonlinear anisotropic, harmonic potential fields: A physical metaphor," *IEEE Trans. Syst., Man, Cybern. A*, vol. 32, no. 6, pp. 705–723, Nov. 2002.
[4] S. Masoud and A. Masoud, "Constrained motion control using vector potential fields," *IEEE Trans. Syst., Man, Cybern. A*, vol. 30, no. 3, pp. 251–272, May 2000.
[5] A. Masoud, "An informationally-open, organizationally-closed control structure for navigating a robot in an unknown, stationary environment," in *Proc. 2003 IEEE Int. Symp. Intelligent Control*, Houston, TX, Oct. 5–8, 2003, pp. 614–619.
[6] A. Masoud and S. Masoud, "A self-organizing, hybrid, PDE-ODE structure for motion control in informationally-deprived situations," in *Proc. 37th IEEE Conf. Decision and Control*, Tampa, FL, Dec. 16–18, 1998, pp. 2535–2540.
[7] A. Masoud and S. Masoud, "Evolutionary action maps for navigating a robot in an unknown, multidimensional, stationary environment, Part II: Implementation and results," in *Proc. 1997 IEEE Int. Conf. Robotics and Automation*, Albuquerque, NM, Apr. 21–27, 1997, pp. 2090–2096.
[8] A. Masoud, S. Masoud, and M. Bayoumi, "Robot navigation using a pressure generated mechanical stress field, the biharmonic potential approach," in *Proc. 1994 IEEE Int. Conf. Robotics and Automation*, San Diego, CA, May 8–13, 1994, pp. 124–129.
[9] O. Khatib, "Real-time obstacle avoidance for manipulators and mobile robots," in *Proc. IEEE Int. Conf. Robotics and Automation*, St Louis, MO, Mar. 25–28, 1985, pp. 500–505.
[10] X. Yun and K. Tan, "A wall-following method for escaping local minima in potential field based motion planning," in *Proc. 8th Int. Conf. Advanced Robotics (ICAR '97)*, Monterey, CA, July 7–9, 1997, pp. 421–426.
[11] A. Petrov and I. Sirota, "Control of a robot-manipulator with obstacle avoidance under little information about the environment," in *Proc. 8th IFAC Congr.*, Kyoto, Japan, Aug. 1981, vol. 14, pp. 54–59.
[12] B. Krogh, "A generalized potential field approach to obstacle avoidance control," in *Proc. Robotics Research: The Next Five Years and Beyond*, Bethlehem, PA, Aug. 14–16, 1984, pp. 1–15.
[13] D. Koditschek, "Exact robot navigation by means of potential functions: Some topological considerations," in *IEEE Int. Conf. Robotics and Automation*, Raleigh, NC, Mar. 1987, pp. 1–6.
[14] D. Koditschek and E. Rimon, "Exact robot navigation using artificial potential functions," *IEEE Trans. Robot. Automat.*, vol. 8, pp. 501–518, Oct. 1992.
[15] Y. Koren and J. Borenstein, "Potential field methods and their inherent limitations for mobile robot navigation," in *Proc. 1991 IEEE Int. Conf. Robotics and Automation*, Sacramento, CA, Apr. 1991, pp. 1398–1404.
[16] C. Connolly, R. Weiss, and J. Burns, "Path planning using laplace equation," in *Proc. IEEE Int. Conf. Robotics and Automation*, Cincinnati, OH, May 13–18, 1990, pp. 2102–2106.
[17] E. Prassler, "Electrical networks and a connectionist approach to pathfinding," in *Connectionism in Perspective*, R. Pfeifer, Z. Schreter, F. Fogelman, and L. Steels, Eds. Amsterdam, the Netherlands: Elsevier, North-Holland, 1989, pp. 421–428.
[18] I. Tarassenko and A. Blake, "Analogue computation of collision-free paths," in *Proc. IEEE Int. Conf. Robotics and Automation*, Sacramento, CA, Apr. 1991, pp. 540–545.
[19] J. Decuyper and D. Keymeulen, "A reactive robot navigation system based on a fluid dynamics metaphor," in *Proc. Parallel Problem Solving from Nature, First Workshop*, H. Schwefel and R. Hartmanis, Eds. Dortmund, Germany, Oct. 1–3, 1990, pp. 356–362.
[20] S. Akishita, S. Kawamura, and K. Hayashi, "New navigation function utilizing hydrodynamic potential for mobile robot," in *Proc. IEEE Int. Workshop Intelligent Motion Control*, Istanbul, Turkey, Aug. 20–22, 1990, pp. 413–417.
[21] J. Guldner and V. Utkin, "Sliding mode control for gradient tracking and robot navigation using artificial potential fields," *IEEE Trans. Robot. Automat.*, vol. 11, pp. 247–254, Apr. 1995.
[22] A. Masoud, "Using hybrid vector-harmonic potential fields for multi-robot, multi-target navigation in a stationary environment," in *Proc. 1996 IEEE Int. Conf. Robotics and Automation*, Minneapolis, MN, Apr. 22–28, 1996, pp. 3564–3571.
[23] J. LaSalle, "Some extensions of Lyapunov's second method," *IRE Trans. Circuit Theory*, vol. CT-7, no. 4, pp. 520–527, 1960.
[24] J. Milnor, *Morse Theory*. Princeton, NJ: Princeton Univ. Press, 1963.
[25] G. Strang, *Linear Algebra and Its Applications*. New York: Academic Press, 1988.
[26] S. Axler, P. Bourdon, and W. Ramey, *Harmonic Function Theory*, 2nd ed. New York: Springer-Verlag, 2001.
[27] S. Arimoto and F. Miyazaki, "Stability and robustness of PID feedback control for robotics manipulators of sensory capabilities," in *Proc. 1st Int. Symp. Robotics Research*, 1984, pp. 385–407.
[28] V. I. Istratescu, *Fixed Point Theory, An Introduction*. Holland: Reidel, 1981.
[29] H. Lutkepohl, *Handbook on Matrices*. New York: Wiley, 1996.
[30] A. Masoud, "Decentralized, self-organizing, potential field-based control for individually-motivated, mobile agents in a cluttered environment: A vector-harmonic potential field approach," *IEEE Trans. Syst., Man, Cybern. A*, vol. 37, no. 3, pp. 372–390, May 2007.
[31] A. Masoud, "Dynamic trajectory generation for spatially constrained mechanical systems using harmonic potential fields," in *Proc. 2007 IEEE Int. Conf. Robotics and Automation*, Rome, Italy, Apr. 10–14, 2007, pp. 1980–1985.
[32] A. Masoud, "Agile, steady response of inertial, constrained holonomic robots using nonlinear, anisotropic dampening forces," in *Proc. 45th IEEE Conf. Decision and Control*, Manchester Grand Hyatt Hotel, San Diego, CA, Dec.13–15, 2006, pp. 6167–6172.
[33] A. Masoud, "Solving the narrow corridor problem in potential field-guided autonomous robots," in *Proc. 2005 IEEE Int. Conf. Robotics and Automation*, Barcelona, Spain, Apr. 18–22, 2005, pp. 2920–2925.

Ahmad A. Masoud received his B.Sc. degree in electrical engineering with a major in power systems and a minor in communication systems from Yarmouk University, Irbid, Jordan, in 1985, and his M.Sc. and Ph.D. degrees in electrical engineering from Queen's University, Kingston, Ontario, Canada, in 1989 and 1995, respectively. He worked as a researcher with the Electrical Engineering Department, Jordan University of Science and Technology, Irbid, from 1985 to 1987. He was also a part-time assistant professor and a research fellow with the Electrical Engineering Department, Royal Military College of Canada, Kingston, from 1996 to 1998. During that time, he carried out research in digital signal processing-based demodulator design for high-density, multiuser satellite systems and taught courses in robotics and control systems. He is currently an assistant professor with the Electrical Engineering Department, King Fahd University of Petroleum and Minerals, Dhahran, Saudi Arabia. He is a Member of the IEEE. His current interests include navigation and motion planning, robotics, constrained motion control, intelligent control, and DSP applications in machine vision and communication.

Address for Correspondence: Ahmad A. Masoud, Electrical Engineering Department, KFUPM, P.O. Box 287, Dhaharan 31261, Saudi Arabia. E-mail: masoud@kfupm.edu.sa.